Contrib Mineral Petrol (1992) 110:488–499

Contributions to Mineralogy and Petrology

Experimentally determined mineral-melt partition coefficients for Sc, Y and REE for olivine, orthopyroxene, pigeonite, magnetite and ilmenite

Roger L. Nielsen[1], William E. Gallahan[1], Florence Newberger[2]

[1] College of Oceanography, Ocean Admin. 104, Oregon State University, Corvallis, OR 97331-5503, USA
[2] Board of Earth Sciences, University of California, Santa Cruz, Santa Cruz, CA 95064, USA

Received April 10, 1991 / Accepted October 7, 1991

Abstract. Our current lack of understanding of the partitioning behavior of Sc, Y and the REE (rare-earth elements) can be attributed directly to the lack of a sufficiently large or chemically diverse experimental data set. To address this problem, we conducted a series of experiments using several different natural composition lavas, doped with the elements of interest, as starting compositions. Microprobe analyses of orthopyroxene, pigeonite, olivine, magnetite, ilmenite and co-existing glasses in the experimental charges were used to calculate expressions that describe REE partitioning as a function of a variety of system parameters. Using expressions that represent mineral-melt reactions (versus element ratio distribution coefficients) it is possible to calculate terms that express low-Ca pyroxene-melt partitioning behavior and are independent of both pyroxene and melt composition. Compositional variations suggest that Sc substitution in olivine involves either a paired substitution with Al or, more commonly, with vacancies. The partitioning of Sc is dependent both on melt composition and temperature. Our experimentally determined olivine-melt REE Ds (partition coefficients) are similar to, but slightly higher than those reported by McKay (1986) and support their conclusions that olivines are strongly LREE depleted. Y and REE mineral/melt partition coefficients for magnetite range from 0.003 for La to 0.02 for Lu. Ilmenite partition coefficients range from 0.007 for La to 0.029 for Lu. These experimental values are two orders of magnitude lower than many of the published values determined by phenocryst/matrix separation techniques.

Introduction

A set of parameters that describe the mineral-melt partitioning behavior of the elements of interest is common to all models of igneous differentiation. Whether these expressions are partition coefficients, empirical parameters, or equilibrium constants, the applicability and accuracy of any description of partitioning behavior is dependent upon the quality and quantity of the experimental data on which it is based.

The experimental data base on the partitioning of the rare-earth elements (REE) between pigeonite, orthopyroxene, olivine, magnetite, ilmenite and natural terrestrial silicate melts is limited in its range of temperature and composition, and totally lacking for some systems. The existing data set is of high quality, but is largely restricted to lunar, meteoritic or synthetic systems. In addition, generally no distinction is made between orthopyroxene and pigeonite.

The majority of the mineral-melt partitioning data that currently are being used by petrologists for modeling mafic to intermediate composition systems were determined by phenocryst separation and analysis. This body of data exhibits many of the problems that are associated with that technique. In particular, because low-Ca pyroxene, olivine and oxide-melt partition coefficients for Y and the REE are small for mafic systems, the phenocryst/matrix determinations are highly susceptible to contamination of the phenocryst separates by glass and trace phases (McKay 1986). Reported values for the partition coefficients for magnetite, cover a range of two orders of magnitude for individual REE in geochemically similar systems. For example, a D_{La} of 0.02 was reported for basaltic liquids by Lemarchande et al. (1987), as opposed to a value of 3.0 reported by Schock (1979). Consequently, the relevance of any calculations made using those partition coefficients is suspect.

This state of affairs exists in spite of the fact that the REE are one of the most commonly used groups of trace elements in petrology. The goal of this investigation was to expand the experimental data base for terrestrial basaltic to dacitic systems, and to constrain the effect of phase composition and temperature on the partitioning behavior of Y, Sc and the REE in common liquidus phases. We have included Y because of its similar behavior to the heavy rare earths (HREE), and Sc

Offprint request to: R.L. Nielsen

because it is another trivalent cation of potential importance, the details of whose behavior is largely unknown.

Experimental and analytical procedures

The starting compositions were selected on the basis of two criteria, first that they be natural lavas saturated near the liquidus at one atmosphere with olivine, pyroxene, and/or oxides, and second, that the liquids produced cover the widest possible range of composition. The starting compositions range from hawaiian tholeiites to arc andesites (Table 1). The rocks that were the source of the starting compositions were powdered and doped with Sc, Y, and the REE as oxide powders at two different concentration levels (0.5 and 2.0 wt%). Mixtures were ground as acetone slurries, using an alumina mortar and pestle, then fused in graphite crucibles in a controlled atmosphere set at the QFM (quartz-fayalite-magnetite) buffer. The compositions were then re-crushed and re-fused. Two separate groupings of trace elements, one with Sc, Y, and La, and the other with Sm, Gd, and Ho or Lu, were prepared to avoid overlapping X-ray lines (e.g., La and Sm L-lines).

Charges of the doped glasses were suspended in a 1 atmosphere Deltech vertical quench, gas mixing furnace, using thin (0.003 inch) Pt wire loops in order to reduce Fe loss. Experimental charges were raised above their liquidi for 2–4 h to assure melt homogeneity, then cooled to run temperatures at a rate greater than 500° C/h, held for 1–14 days, and water quenched. Temperatures were measured using a $Pt-Pt_{90}Rh_{10}$ thermocouple calibrated against the melting point of gold. Oxygen fugacities were monitored with an oxygen electrolyte cell (Williams and Mullins 1981) calibrated at the iron-wustite buffer. Mixtures of H_2 and CO_2 buffered the oxygen fugacities at the QFM buffer.

Major, minor, and trace elements were analyzed by electron microprobe (Cameca SX-50 at OSU) in two different ways, depending on the concentration of the element. For the major elements X-ray intensities were measured at 15 kV accelerating potential and 20 nA beam current. A defocused beam, (5–10 μm diameter) was used to minimize beam damage. Counting times (on-peak) were: 10 s for major and minor elements, 50 s for Sc, and 100 s for Y, Gd, Ho and Lu in pyroxene. Background counts were taken above and below the peak for 1/2 the on-peak counting time (e.g., 25 s for Sc). Correction of X-ray intensities for deadtime, background, and matrix effects was made using the Cameca PAP routine. Most analyses for mineral-melt pairs were averaged from line traverses containing three to five analyzed points in each phase. In order better to assure an equilibrium mineral-melt pair, pyroxene and glass analyses were taken in close proximity to one another.

Because of the general incompatibility of these elements in pyroxene, olivine and oxides, their concentration can be near the detection limits for the electron microprobe. In order to maximize the precision and accuracy of our analyses at low concentrations (< 500 ppm), we adopted a variant of the technique of McKay (1986). X-ray intensities were measured at the peak wavelength for counting timnes of 1000 s then at 4 different background offsets on each side of the peak, again for 1000 s each. Beam current was increased to 100 nA. Net intensities ($I_{peak}-I_{background}$) in total counts were calculated for mineral and glass. The ratio of the intensities, $I^{cpx}_{net}/I^{glass}_{net}$ was assumed to be the partition coefficient. Several analyses were made using this technique and, for comparison, others were made using the CAMECA PAP correction on charges with moderate levels of REE. Confirming the conclusions of Colson et al. (1988), we found that the error due to the lack of a matrix correction was smaller (2–4% relative) than the analytical precision.

K_2O was included in the analytical routine for the mineral phases. Because of potassium's incompatibility in any of the phases of interest at low pressure, it was used as an indicator of glass inclusions. Analyses were done only on crystals > 50 μm in diameter. In some of these charges, particularly Hakone old Sonoma, crystal size was generally less than 50 μm. In addition, because of a lack of 3D information, it is possible that there was some glass fluorescence in these analyses. Therefore, low distribution coefficients (e.g., below ~0.001) should be considered maximum values, with the effect becoming more important as D becomes smaller. Mineral analyses containing $K_2O > 0.05$ wt% were excluded from the data set.

Minor quench growth of olivine was detected optically in approximately 20% of the run products. To avoid the concentration gradients associated with these quench olivines (Kring and McKay 1984), analyses were restricted to minerals and glasses at least 30 μm from any phase boundary.

In the majority of experimental studies, some method of doping

Table 1. Starting compositions

	H87-3	43152	3/83	KL77	E-1	GC-68	ML-176	TLW67	HOS
SiO_2	47.66	49.15	50.90	51.34	47.4	49.46	52.11	51.00	55.83
TiO_2	2.42	3.76	3.01	3.69	2.2	4.28	2.09	3.49	0.61
Al_2O_3	12.35	11.27	14.29	13.65	11.5	14.09	13.81	13.85	17.75
Fe_2O_3	1.38	–	1.54	1.86	3.7	–	–	2.26	2.76
FeO	10.04	18.66	10.08	10.55	8.8	12.47	11.03	10.21	6.01
MnO	0.17	–	0.17	0.18	0.18	0.22	0.18	0.18	–
MgO	11.44	4.21	6.04	5.28	13.0	4.62	6.68	5.54	3.90
CaO	11.51	9.33	10.34	9.27	10.4	9.63	10.63	9.53	8.62
Na_2O	2.18	2.48	2.59	2.82	2.0	3.03	2.40	2.74	2.98
K_2O	0.57	0.19	0.61	0.79	0.37	1.18	0.40	0.77	0.55
P_2O_5	0.29	0.31	0.32	0.40	0.29	1.02	0.26	0.40	–
Reference	3	1	4	2	5	6	7	8	9

1. Galapagos ferrobasalt – Melson (personal communication)
2. Kilauca tholeiite – Moore et al. (1980)
3. Mauna Kea ankaramite – Porter et al. (1987)
4. Kilauea tholeiite – Neal et al. (1988)
5. Uwekahuna Bluff picrite – Casadevall and Dzurisin (1987)
6. Mauna Loa tholeiite-electron microprobe analysis of fused glass beads – unpublished
7. Mauna Loa tholeiite – Rhodes (1988)
8. Kilauea tholeiite – Wright and Fiske (1971)
9. Hakone Old Sonoma augite-hypersthene andesite – Kuno (1950)

is used. The trace element of interest is added to the charge in sufficient concentration to facilitate electron microprobe analyses (Leeman 1974; Lindstrom 1976; Ray et al. 1983; Colson et al. 1988; McKay 1986; McKay et al. 1986a; Dunn 1987). Because these doping levels are usually in the wt% range, several orders of magnitude higher than the concentration in natural systems, there is no guarantee that the results of the experiments will be relevant to the modeling of natural systems. Watson (1985) and McKay (1986) present extensive arguments in support of the contention that experimentally determined trace element partitioning is constant from natural concentration levels to doped levels (~1–3 wt%). No evidence of an upper limit to Henry's Law is apparent for most systems. This has been confirmed for olivine and orthopyroxene-melt partition coefficients by ion-probe work performed by Beattie (1991). Nevertheless, the responsibility remains for the experimentalist to show that partitioning behavior is independent of the dopant levels in each study.

To evaluate the dependence of pyroxene-melt partition coefficients on elemental concentrations (possible Henry's Law violation), a series of experiments on a single system were conducted at several different doping levels. The results, reported in Gallahan and Nielsen (in press), indicated consistent partitioning behavior over the concentration range of 0.05–2 mol% REE in the melt. In addition, the partition coefficients derived from these experiments are comparable to published data for natural concentrations (e.g., Johnson 1989). From these results, and those of Beattie (1991), it can be inferred that the experiments were conducted within the Henry's Law limits and are applicable to systems at natural concentrations. A detailed evaluation of the Henry's Law limit for Sc in olivine is presented in a later section.

Results

The experimental results and run conditions for this investigation (Tables 2 and 4) represent averages of at least three analyzed points on each phase in co-existing mineral-melt pairs. Standard deviation is presented in tables 2 and 4 the form of a 1 σ sample standard deviation calculated from analyes of individual mineral-melt pairs. For major components (e.g., Mg, Al, Si, Ca, Fe), glass, olivine, magnetite and ilmenite are homogeneous within 3% relative. Low-Ca pyroxenes are homogeneous within approximately 5%. Trace-element precisions range from 3–5% for the HREE in pigeonite to >20% for La in orthopyroxene, olivine and the oxides.

The liquid compositions cover a large range of natural magmas in equilibrium with low-Ca pyroxene at low pressure (Fig. 1). Included for comparison are the liquid compositions from the experiments of Colson et al. (1988) and McKay et al. (1986a). Any relationship that can be derived from this data set to describe the partitioning of these elements should be applicable to virtually all low-pressure models of lunar and terrestrial petrogenesis.

Pyroxene

The most commonly applied parameter to describe trace-element mineral-melt partitioning is the concentration-ratio partition coefficient. Based upon their results on the Shergottite starting composition, McKay et al. (1986) found a strong correlation between low-Ca pyroxene partition coefficients with the wollastonite content

Table 2a. Experimentally determined pyroxene compositions. All concentrations are expressed in terms of cation normalized mole percents. (Cation normalized analysis of anorthite is 20 Ca, 40 Al and 40 Si). Glasses in 2b correspond to pyroxenes in 2a. 1 σ standard deviation given in parentheses (e.g., 1.01(4) is 1.01 ± 0.04)

System	T (C)	Na	Mg	Al	Si	Ca	Ti	Cr	Mn	Fe	Sm	Gd	Ho	Lu
H.O.S.	1090	0.06(3)	33.9(3)	1.1(1)	48.7(4)	2.0(2)	0.17(3)	0.02(0)	0.38(5)	13.4(2)	0.04(1)	0.06(1)	0.15(3)	0.00(0)
H.O.S.	1090	0.15(8)	34.0(2)	2.1(5)	47.9(9)	2.4(3)	0.23(4)	0.04(1)	0.35(4)	12.5(1)	0.07(2)	0.10(2)	0.24(5)	0.00(0)
H.O.S.	1090	0.07(4)	34.6(6)	1.7(2)	48.5(6)	1.8(2)	0.17(3)	0.04(1)	0.35(4)	12.5(6)	0.04(1)	0.06(1)	0.19(4)	0.00(0)
H.O.S.	1090	0.12(6)	33.5(4)	1.9(2)	48.3(4)	2.5(1)	0.21(4)	0.02(0)	0.37(4)	12.7(3)	0.05(1)	0.08(2)	0.23(5)	0.00(0)
H.O.S.	1080	0.06(3)	32.0(5)	2.5(3)	47.7(8)	2.5(3)	0.32(6)	0.00(0)	0.36(4)	14.2(2)	0.06(1)	0.11(2)	0.20(4)	0.00(0)
H.O.S.	1080	0.11(6)	32.6(2)	1.6(2)	47.8(4)	2.2(2)	0.18(3)	0.04(1)	0.39(5)	14.8(4)	0.05(1)	0.07(1)	0.20(4)	0.00(0)
H.O.S.	1080	0.17(9)	32.4(6)	2.5(4)	47.4(3)	2.4(3)	0.25(5)	0.05(1)	0.26(3)	14.4(2)	0.05(1)	0.09(2)	0.19(4)	0.00(0)
KL-77-5	1076	0.07(4)	30.7(4)	0.7(1)	49.3(1)	3.9(5)	0.36(6)	0.01(0)	0.28(3)	14.5(2)	0.03(1)	0.03(1)	0.00(0)	0.07(2)
E-1	1110	0.22(4)	35.7(7)	1.6(2)	48.1(5)	4.8(6)	0.42(8)	0.29(6)	0.27(3)	8.1(4)	0.08(2)	0.12(2)	0.26(5)	0.00(0)
E-1	1105	0.30(6)	33.3(2)	1.9(2)	48.4(9)	6.6(8)	0.43(8)	0.31(6)	0.26(3)	8.1(1)	0.12(2)	0.14(3)	0.27(5)	0.00(0)
E-1	1100	0.07(1)	34.3(9)	1.3(3)	47.6(7)	4.5(5)	0.63(11)	0.08(2)	0.24(3)	11.2(4)	0.02(1)	0.02(1)	0.05(1)	0.00(0)
GC-68-5	1080	0.25(5)	29.9(1)	1.0(1)	48.8(5)	6.8(8)	0.67(12)	0.00(0)	0.34(4)	12.1(2)	0.04(1)	0.05(1)	0.09(2)	0.00(0)
ML-176	1090	0.14(3)	30.4(2)	1.5(2)	48.3(3)	5.5(7)	0.45(8)	0.06(1)	0.29(3)	13.1(2)	0.06(1)	0.09(2)	0.18(4)	0.00(0)
TLW-67	1100	0.21(4)	29.6(9)	2.0(2)	48.4(4)	8.6(2)	0.63(11)	0.07(1)	0.22(3)	9.9(1)	0.10(2)	0.10(2)	0.00(0)	0.21(4)
TLW-67	1120	0.26(5)	29.9(1)	1.2(1)	48.7(2)	10.9(3)	0.53(10)	0.12(2)	0.22(3)	8.0(1)	0.03(1)	0.03(1)	0.00(0)	0.06(1)
TLW-67	1120	0.27(5)	27.5(9)	1.3(3)	49.0(5)	13.6(6)	0.56(10)	0.07(1)	0.25(3)	7.3(2)	0.03(1)	0.05(1)	0.00(0)	0.07(1)

System	T (C)	Na	Mg	Al	Si	Ca	Ti	Cr	Mn	Fe	Sc	Y	La
43152	1050	0.88(9)	15.7(1)	3.0(3)	48.3(3)	6.9(8)	0.59(6)	0.00(0)	0.54(3)	21.0(3)	3.05(6)	0.00(0)	0.030(3)
43152	1100	0.30(3)	24.9(2)	2.1(2)	48.3(4)	7.9(9)	0.59(11)	0.00(0)	0.37(4)	14.8(4)	0.71(4)	0.04(1)	0.003(1)
43152	1080	0.46(5)	24.8(1)	2.0(2)	48.5(8)	5.4(7)	0.34(6)	0.00(0)	0.43(5)	16.1(2)	1.84(17)	0.05(1)	0.002(1)
H.O.S.	1090	0.48(5)	30.2(4)	4.4(5)	47.8(5)	3.0(4)	0.32(6)	0.03(3)	0.31(1)	11.5(5)	1.98(11)	0.24(5)	0.030(2)
H.O.S.	1090	0.28(3)	32.2(2)	2.4(3)	48.2(4)	2.5(3)	0.21(4)	0.04(1)	0.34(4)	12.4(2)	1.33(7)	0.15(3)	0.030(4)
H.O.S.	1080	0.15(2)	29.3(2)	3.0(3)	47.4(1)	2.8(3)	0.07(1)	0.05(3)	0.28(3)	15.4(1)	1.46(9)	0.13(3)	0.020(4)
H.O.S.	1080	0.14(1)	30.9(2)	1.9(2)	48.2(2)	2.9(1)	0.02(1)	0.04(2)	0.34(4)	14.5(3)	1.00(2)	0.09(2)	0.007(1)
H.O.S.	1080	0.17(2)	30.7(3)	2.3(3)	47.9(1)	2.5(3)	0.03(1)	0.04(2)	0.31(1)	14.7(2)	1.10(2)	0.08(2)	0.030(1)
H.O.S.	1105	0.28(3)	32.1(2)	3.5(4)	47.1(9)	2.7(2)	0.19(3)	0.05(1)	0.36(4)	11.8(4)	2.20(4)	0.21(4)	0.020(2)
H.O.S.	1105	0.27(3)	32.0(2)	3.0(3)	47.9(3)	2.3(2)	0.21(4)	0.08(2)	0.31(3)	12.1(1)	1.73(5)	0.13(3)	0.001(1)
H.O.S.	1110	0.18(2)	33.4(5)	2.5(3)	47.5(4)	2.2(3)	0.18(3)	0.07(1)	0.30(5)	12.1(2)	1.46(9)	0.13(3)	0.010(1)
H.O.S.	1110	0.19(2)	33.4(2)	2.6(3)	47.6(5)	1.9(2)	0.18(3)	0.06(1)	0.33(2)	12.2(1)	1.43(9)	0.11(2)	0.010(1)
3/83KE2	1100	0.16(2)	31.0(2)	1.0(1)	49.1(1)	3.6(4)	0.37(7)	0.00(0)	0.27(3)	14.0(2)	0.41(8)	0.02(1)	0.008(1)
KL-77-5	1090	0.75(8)	25.0(4)	3.9(4)	47.0(4)	7.8(2)	0.64(8)	0.00(0)	0.23(1)	11.6(1)	2.90(8)	0.24(5)	0.010(2)
KL-77-5	1090	0.95(6)	24.4(1)	3.3(4)	46.8(3)	10.0(3)	0.71(3)	0.05(3)	0.21(4)	10.2(3)	2.89(8)	0.30(6)	0.020(2)
GC-68-5	1100	0.20(2)	33.5(2)	1.8(2)	48.4(4)	4.0(5)	0.58(2)	0.12(2)	0.19(2)	10.5(1)	0.68(4)	0.09(2)	0.000(0)

Table 2b. Experimental glass compositions. All are in terms of cation normalized mole percent

	T (C)	Na	Mg	Al	Si	P	K	Ca	Ti	Mn	Fe	Sm	Gd	Ho	Lu
H.O.S.	1090	4.0(2)	5.1(3)	14.5(1)	56.4(3)	0.09(3)	1.4(2)	6.0(1)	1.13(11)	0.12(2)	7.8(2)	1.06(6)	1.12(3)	1.28(5)	0.0(0)
H.O.S.	1090	4.0(2)	5.2(3)	14.3(2)	55.6(5)	0.18(4)	1.3(1)	6.2(2)	1.15(12)	0.17(3)	8.1(4)	1.11(5)	1.20(3)	1.42(7)	0.0(0)
H.O.S.	1090	4.1(2)	5.0(2)	14.2(3)	56.2(4)	0.18(4)	1.3(1)	6.1(1)	1.08(13)	0.17(3)	8.1(2)	1.09(2)	1.13(7)	1.34(5)	0.0(0)
H.O.S.	1090	3.7(1)	5.0(3)	14.4(2)	56.7(4)	0.13(3)	1.4(1)	6.0(3)	1.14(17)	0.21(4)	8.1(3)	1.04(7)	1.04(5)	1.25(4)	0.0(0)
H.O.S.	1080	3.2(2)	4.6(2)	14.1(2)	57.2(3)	0.19(6)	1.4(2)	6.1(1)	1.19(12)	0.19(4)	8.4(2)	1.10(9)	1.11(3)	1.23(2)	0.0(0)
H.O.S.	1080	3.4(1)	4.8(2)	13.7(1)	55.8(6)	0.25(5)	1.3(1)	6.2(3)	1.24(16)	0.17(3)	9.3(2)	1.24(7)	1.27(2)	1.33(9)	0.0(0)
H.O.S.	1080	3.3(2)	4.8(2)	14.5(1)	55.8(4)	0.23(5)	1.3(1)	6.3(3)	1.16(12)	0.14(4)	9.0(5)	1.13(2)	1.15(8)	1.24(8)	0.0(0)
KL-77-5	1076	4.2(2)	6.1(3)	11.5(2)	47.3(3)	0.65(8)	1.4(1)	8.7(2)	4.07(11)	0.20(2)	13.0(3)	0.97(3)	0.90(2)	0.0(0)	0.95(5)
E-1	1100	4.5(2)	8.5(4)	12.6(1)	48.7(3)	0.30(6)	0.8(1)	8.1(2)	3.81(18)	0.12(2)	6.9(1)	1.77(7)	1.78(8)	2.02(3)	0.0(0)
E-1	1100	4.9(2)	8.0(4)	13.0(2)	49.5(1)	0.23(5)	0.8(1)	8.0(2)	3.20(12)	0.12(2)	7.4(1)	1.49(4)	1.54(5)	1.76(4)	0.0(0)
E-1	1100	5.1(3)	6.8(3)	14.1(1)	49.8(2)	0.55(9)	1.7(2)	8.3(1)	4.21(12)	0.14(4)	7.9(2)	0.43(5)	0.43(2)	0.46(1)	0.0(0)
GC-68-5	1080	5.3(3)	4.6(3)	15.3(2)	53.6(3)	0.92(5)	3.2(3)	6.2(3)	2.74(17)	0.15(2)	7.5(1)	0.60(2)	0.63(5)	0.61(6)	0.0(0)
ML-176	1090	3.7(2)	6.7(3)	11.9(1)	48.2(4)	0.39(8)	0.8(1)	9.1(2)	3.01(20)	0.16(3)	11.9(2)	1.27(5)	1.29(3)	1.50(2)	0.0(0)
TLW-67	1100	4.1(2)	7.5(4)	13.4(2)	47.4(3)	0.44(9)	1.1(1)	9.2(1)	3.34(13)	0.15(2)	11.1(5)	0.84(8)	0.76(5)	0.0(0)	0.83(3)
TLW-67	1120	5.3(3)	7.7(4)	14.7(1)	49.6(5)	0.37(3)	1.0(2)	8.9(2)	2.99(10)	0.15(2)	8.7(2)	0.19(5)	0.22(4)	0.0(0)	0.21(5)
TLW-67	1120	5.3(3)	7.7(4)	14.7(1)	49.6(3)	0.37(7)	1.0(1)	8.9(2)	2.99(12)	0.15(1)	8.7(2)	0.22(5)	0.23(2)	0.0(0)	0.24(3)

	T (C)	Na	Mg	Al	Si	P	K	Ca	Ti	Mn	Fe	Sc	Y	La
43152	1050	4.6(2)	3.4(5)	10.9(1)	49.4(3)	0.86(4)	0.9(1)	7.2(4)	2.47(11)	0.29(3)	17.3(2)	1.73(2)	0.0(0)	0.99(1)
43152	1100	4.8(3)	6.4(3)	12.3(3)	46.6(4)	0.39(8)	0.3(1)	9.7(5)	3.05(9)	0.28(4)	15.4(3)	0.41(3)	0.16(0)	0.13(0)
43152	1080	4.4(2)	6.2(4)	11.2(2)	45.4(3)	0.36(7)	0.3(1)	8.6(4)	3.36(11)	0.26(6)	16.6(3)	1.93(9)	0.72(1)	0.72(5)
H.O.S.	1090	4.7(3)	4.7(2)	14.4(3)	57.1(6)	0.16(3)	1.5(2)	6.3(3)	1.23(9)	0.16(4)	6.8(1)	0.90(7)	0.96(4)	1.11(8)
H.O.S.	1090	3.8(2)	4.8(1)	14.3(1)	57.6(2)	0.19(4)	1.6(2)	6.4(3)	1.26(13)	0.16(6)	6.8(1)	0.89(3)	1.01(3)	1.17(8)
H.O.S.	1080	3.6(2)	4.4(2)	13.7(1)	56.7(3)	0.27(5)	1.5(1)	6.3(5)	1.34(12)	0.23(2)	8.0(2)	1.72(5)	1.04(2)	1.33(9)
H.O.S.	1080	3.6(1)	4.4(1)	13.7(1)	56.7(3)	0.27(5)	1.5(1)	6.3(3)	1.34(17)	0.23(2)	8.0(2)	1.72(5)	1.04(2)	1.33(9)
H.O.S.	1080	3.4(2)	4.5(2)	14.2(2)	57.1(4)	0.20(4)	1.6(2)	6.4(3)	1.32(6)	0.18(1)	8.1(1)	0.96(3)	0.82(1)	1.26(9)
H.O.S.	1105	3.3(1)	6.5(3)	14.3(1)	55.4(3)	0.13(3)	1.3(1)	6.5(2)	1.02(3)	0.15(5)	8.1(2)	1.01(5)	1.28(6)	0.95(7)
H.O.S.	1105	3.8(1)	5.6(2)	14.7(2)	55.4(2)	0.14(3)	1.4(1)	6.5(3)	1.11(6)	0.15(5)	8.0(3)	1.01(3)	1.32(5)	0.98(7)
H.O.S.	1110	3.9(2)	5.6(3)	15.1(1)	55.1(3)	0.16(3)	1.3(1)	6.7(1)	0.95(4)	0.14(4)	7.7(2)	1.08(7)	1.31(2)	0.92(6)
H.O.S.	1110	3.9(3)	5.0(2)	15.8(1)	55.8(1)	0.12(2)	1.4(1)	6.5(3)	0.92 (9)	0.15(5)	7.5(1)	0.96(8)	1.18(1)	0.80(6)
3/83KE2	1100	4.4(2)	7.1(4)	12.6(2)	47.2(3)	0.46(9)	1.0(1)	9.2(5)	4.16(8)	0.16(1)	12.4(3)	0.59(2)	0.39(3)	0.31(2)
KL-77-5	1090	4.7(2)	8.0(2)	13.1(1)	47.0(6)	0.30(6)	1.2(1)	8.5(4)	2.72(17)	0.12(2)	10.6(2)	1.96(2)	1.08(4)	0.64(4)
KL-77-5	1090	4.5(2)	7.2(4)	12.8(2)	46.6(3)	0.50(8)	1.2(1)	8.1(4)	3.58(10)	0.15(5)	11.5(3)	1.74(2)	1.40(6)	0.90(6)
GC-68-5	1100	4.9(1)	7.7(3)	13.7(1)	47.6(4)	0.90(9)	1.5(1)	8.6(4)	4.43(14)	0.12(2)	8.2(1)	0.67(3)	1.03(9)	0.72(5)

of the pyroxene (Fig. 2). One characteristic that is apparent from a combined data set is that in general the D increases as a function of Ca content in the pyroxene, however there is no single trend. In order to distinguish orthopyroxene from pigeonite, thin sections were made of the experimental charges from this study so that they could be distinguished optically. As one might predict, the distribution at low Ca are orthopyroxene-melt pairs, and those at higher Ca are pigeonite-melt pairs. The pyroxene types in the Colson et al. (1988) and McKay et al. (1986a) data sets were not determined, however one can infer that the Colson et al. (1988) pyroxenes were orthopyroxene, and the McKay et al. (1986a) data were pigeonite. We shall assume this interpretation for the following discussion.

In spite of the presence of two different distributions in the data, both have consistent linear relationships with the Ca content of the pyroxene. The distribution of pigeonite and sub-calcic augite Ds for the data of McKay et al. (1986a) is lower at a given Ca content than the results of this study. This could be due to differences in a number of parameters such as temperature (McKay et al. 1986a at 1140–70° C), melt composition (Fig. 2) or inter-laboratory analytical differences. For Lu and Yb, all data from both elements are shown. This is based on the assumption that these two contiguous elements will have virtually identical partitioning behavior.

An attempt to reduce the compositional effects on partitioning behavior was made by applying the two-lattice melt component activity model of Nielsen (1985) to the data. This model, based upon a modification of the melt model of Bottinga and Weill (1972), assumes that the melt consists of two quasi-lattices, the network formers and the network modifiers. If one assumes that cations mix ideally within each of these quasi-lattices, with no mixing between quasi-lattices, the activity of a component can be calculated as the mole fraction of the component in the quasi-lattice. Application of this model has significantly reduced the compositional dependence of mineral-melt expressions in several other systems (Nielsen 1988).

The results from this application, expressed in terms of compensated partition coefficients (d*) are not greatly different from the distribution of Ds (Fig. 3). However, the differences between the data from the data of McKay et al. (1986a) and that of this study are less. Nevertheless the existence of a strong dependence on the Ca content of the pyroxene remains.

According to the basic principles of equilibrium thermodynamics, the equilibrium constant for a reaction is not dependent on the concentration of any component. A prerequisite of the formulation and application of such a reaction to multicomponent natural systems is some method for calculating the activities of the mineral and

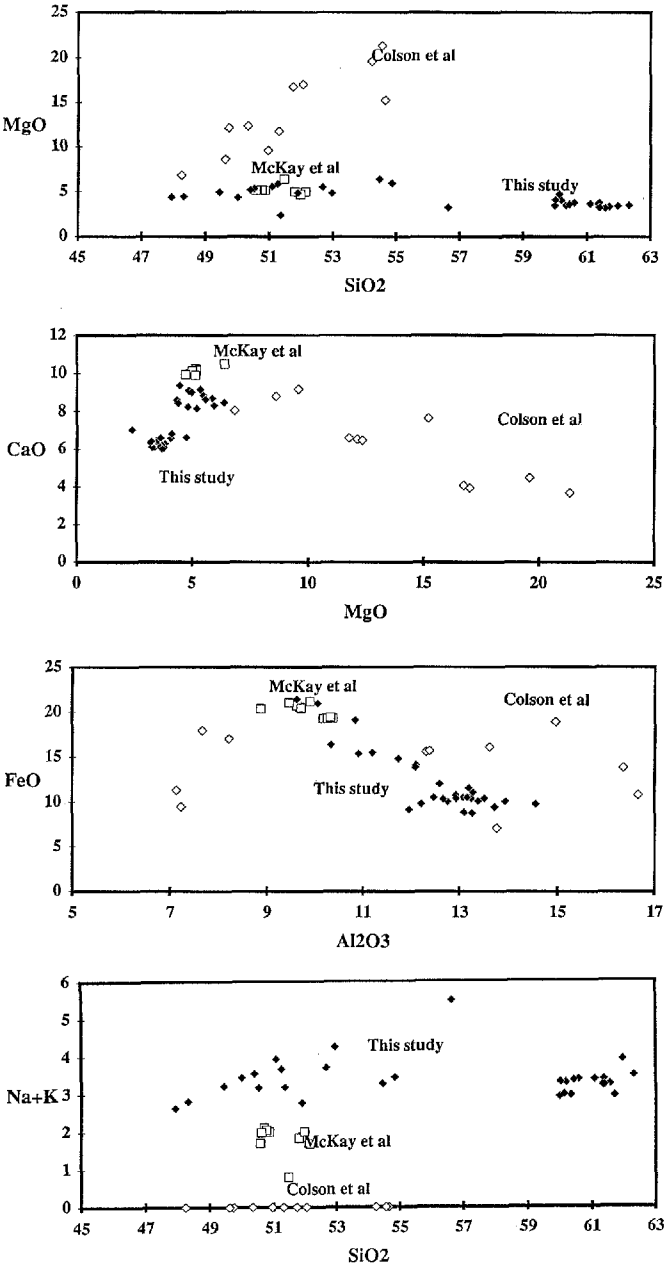

Fig. 1. Glass compositions from low-Ca pyroxene-melt experiments. Included for comparison are the data of McKay et al. 1986a on a Shergottite composition, *squares*, and data on a Ca–Mg–Al–Si–Fe–O synthetic system (Colson et al. 1988, *open diamonds*)

melt components, and knowledge of how the elements of interest are incorporated in the mineral phase. In their study of the partitioning of trivalent cations in low-Ca pyroxenes, Colson et al. (1989) demonstrated that the most likely substitution mechanism for Sc and the REE in pyroxene is in paired substitution with Al. This was confirmed for high-Ca pyroxene (cpx) by Gallahan and Nielsen (in press). This information was used to construct an expression that approximated an equilibrium constant (K) by combining terms for the Al and Si melt components:

$$\mathrm{REEO}_{1.5}(\mathrm{l}) + \mathrm{FMO}(\mathrm{l}) + \mathrm{AlO}_{1.5}(\mathrm{l}) + \mathrm{SiO}_2(\mathrm{l}) = \mathrm{REEFMAlSiO}_6(\mathrm{cpx}) \quad (1)$$

where FM represents Fe and Mg.

$$K = \left[\frac{a^{\mathrm{cpx}}_{\mathrm{REE}}}{(a^{\mathrm{liquid}}_{\mathrm{REEO}_{1.5}})(a^{\mathrm{liquid}}_{\mathrm{AlO}_{1.5}})(a^{\mathrm{liquid}}_{\mathrm{SiO}_2})}\right]\left[\frac{a^{\mathrm{cpx}}_{\mathrm{FM}}}{a^{\mathrm{liquid}}_{\mathrm{FMO}}}\right] \quad (2)$$

Rewriting equation 2, assuming a constant ratio of the activities of Fe and Mg at any temperature:

$$K^* = K \times \left[\frac{a^{\mathrm{liquid}}_{\mathrm{FMO}}}{a^{\mathrm{cpx}}_{\mathrm{FM}}}\right] = \left[\frac{a^{\mathrm{cpx}}_{\mathrm{REE}}}{(a^{\mathrm{liquid}}_{\mathrm{REEO}_{1.5}})(a^{\mathrm{liquid}}_{\mathrm{AlO}_{1.5}})(a^{\mathrm{liquid}}_{\mathrm{SiO}_2})}\right] \quad (3)$$

In making this assumption, we imply that the Fe/Mg exchange is constant at any temperature. This does not assume that the Fe/Me ratio of the individual phases is constant. We do however recognize that the Fe/Mg exchange may vary as a function of composition and that this simplifying assumption may be inaccurate in either Mg- or Fe-rich systems.

Values of K* were calculated from the experimental data and correlated with temperature and a variety of mineral and melt parameters. For pyroxenes with wollastonite contents greater than 30% (0.15 mole fraction Ca), the dependence of K* on Ca content is small (Gallahan and Nielsen, in press). In contrast, the correlation with Ca content for low-Ca pyroxenes (Fig. 4) is strong, confirming the interpretation of McKay et al. (1986a). This would suggest that K* is not an accurate means of estimating REE mineral-melt equilibria over the full range of pyroxene composition. In spite of the strong dependence on Ca, the trends represented by the orthopyroxenes and pigeonites are now co-linear. This allows us to calculate a single expression that describes the partitioning behavior of these elements relevant to both pyroxenes. However, application of these expressions require knowledge of the major-element composition of the pyroxene.

In studies of the partitioning of REE between orthopyroxene and melt, McKay et al. (1986a) and Colson et al. (1988) found a dependence of REE partitioning of the Fe/Mg ratio. Such a correlation is not evident from a combined data set (Fig. 1). This may be due to a variety of factors including the wider range of composition represented in the combined data set. The lack of a clear relationship complicates the search for parameters that can be used for constructing relevant equilibrium expressions, but insures that, once found, expressions will be applicable to a wide range of systems. To incorporate all of the possible compositional dependencies, we derived a set of expressions that include the Fe/Mg exchange together with the demonstrated Ca-REE dependence. One well tested method of deriving compositionally independent mineral-melt expressions is by the use of exchange reactions. Temperature and compositional dependencies will cancel out if the dependencies of the component reactions are proportional to one another (e.g., Fe and Mg in olivine – Roeder and Emslie 1970).

Several attempts were made to derive an expression that was both realistic and was based upon our present understanding of the exchange mechanism in pyroxene.

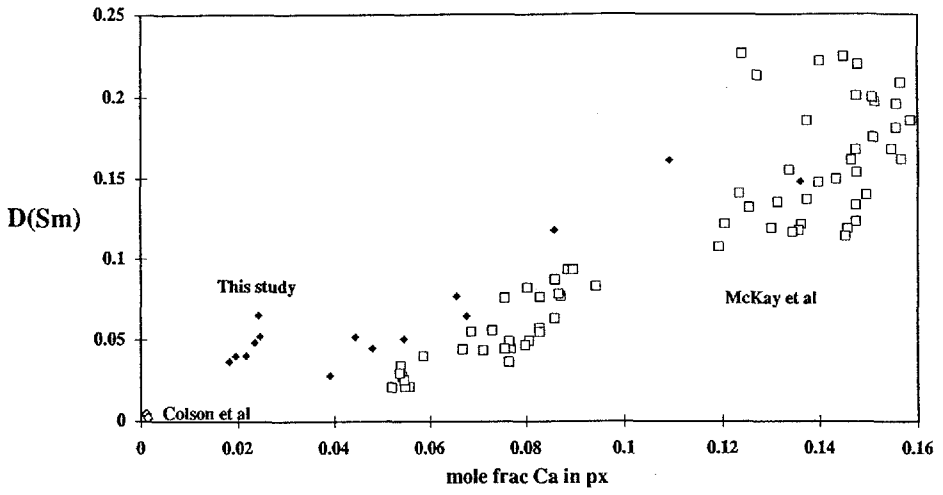

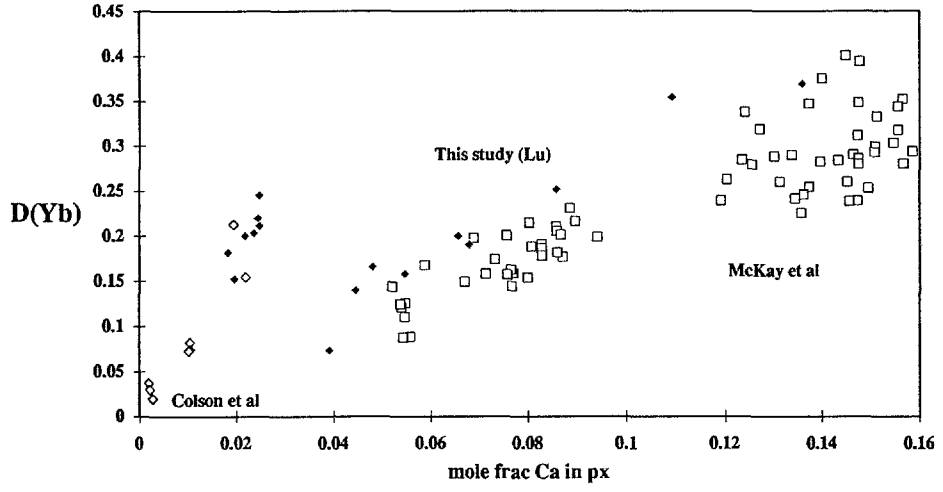

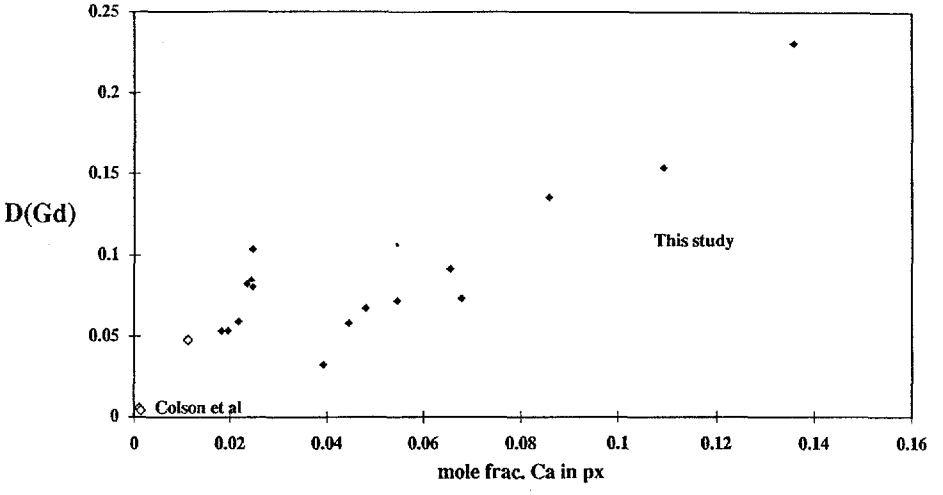

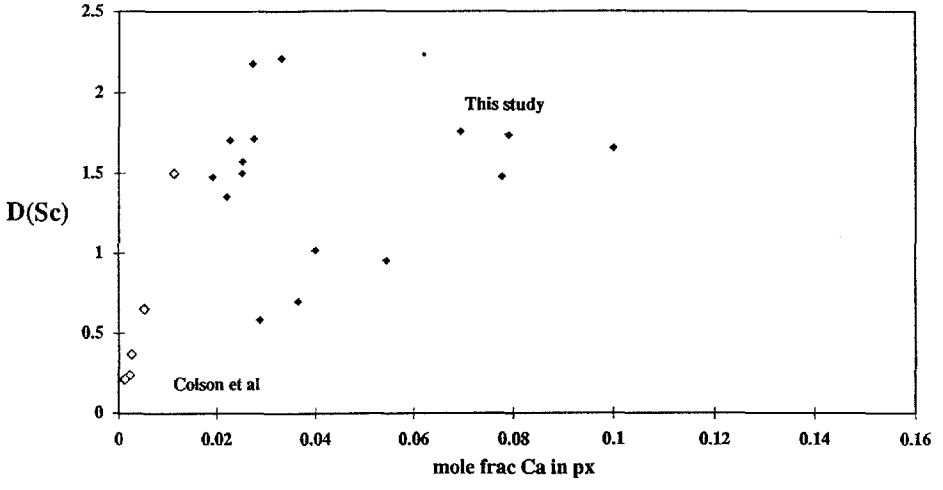

Fig. 2. Low-Ca pyroxene-melt partition coefficients (Ds) for Sc and selected REE. Plot of D_{Yb} includes D_{Ho} and D_{Lu} data from this study. Ds are calculated in terms of ratios of the mole fractions of the cations. Data below 0.03 cation-normalized mole fraction Ca (6% Wo) are orthopyroxene-melt pairs

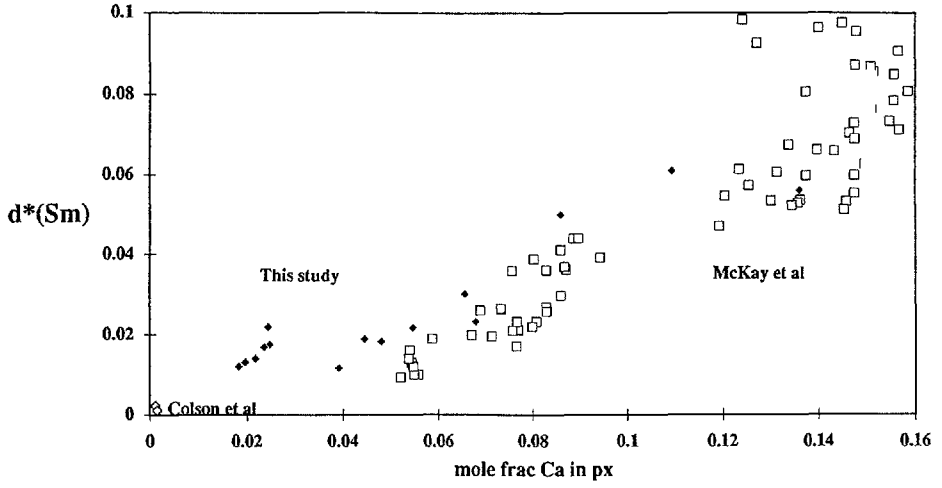

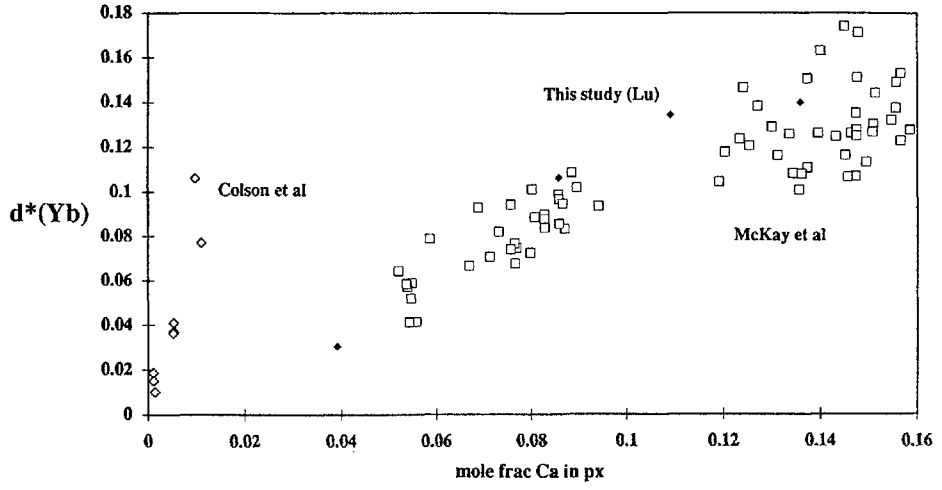

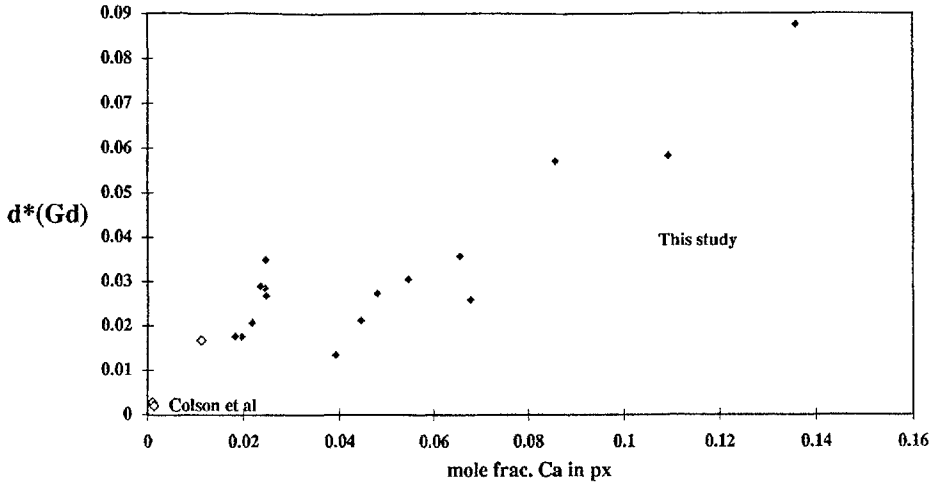

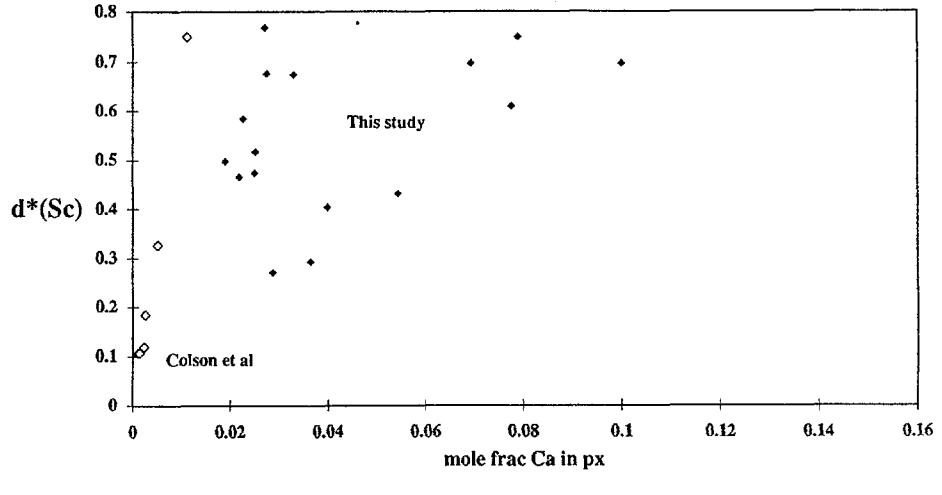

Fig. 3. Low-Ca pyroxene-melt compensated partition coefficients as calculated using the two-lattice melt model. Data and symbols same as Fig. 2

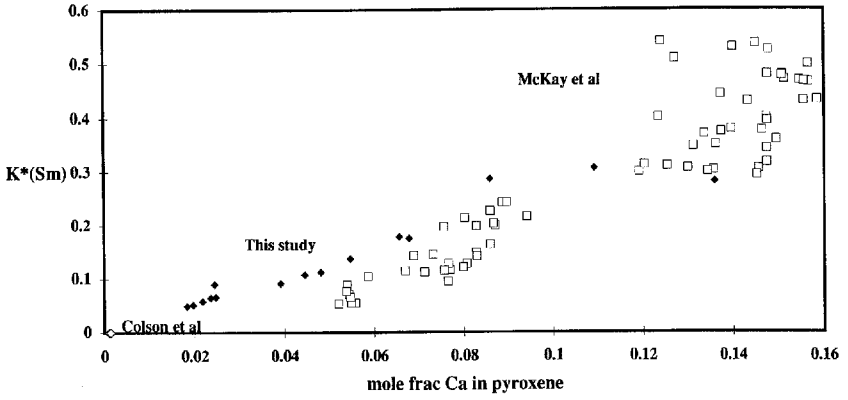

Fig. 4. Correlation of Ca in pyroxene and an abbreviated equilibrium constant for low-Ca pyroxene-melt partitioning of Sm. Data and symbols same as Fig. 2

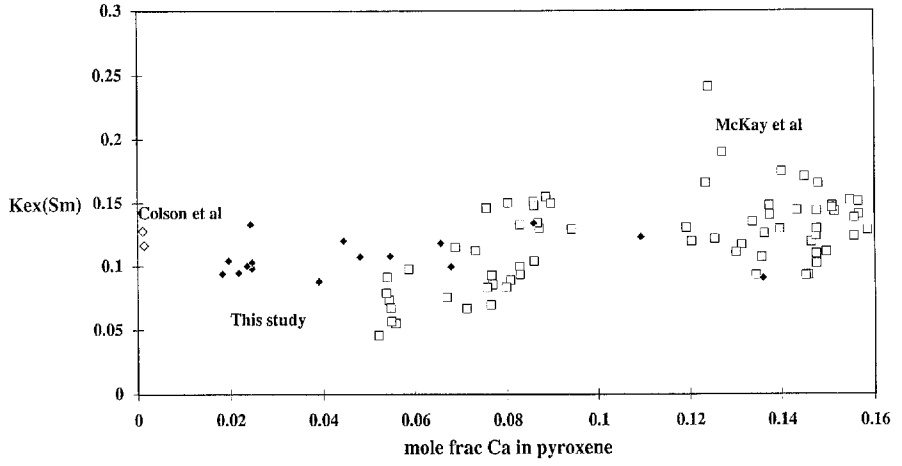

Fig. 5. Equilibrium exchange reaction coefficient for an exchange between $CaMgSi_2O_6$ and $FeSmAlSiO_6$ in equilibrium with melt. Data and symbols same as Fig. 2

The model that produced the data set with the best precision involves an exchange reaction between diopside and a REE–Fe–Al pyroxene component.

$$CaMgSi_2O_6 + REEO_{1.5}(l) + FeO(l) + AlO_{1.5}(l) = REEFeAlSiO_6 + CaO(l) + MgO(l) + SiO_2(l) \quad (4)$$

Since the goal of the investigation is to derive a set of expressions that are accessible to the general petrologic community, and given the lack of evidence for a strong Fe/Mg dependence, we have assumed that the Fe/Mg ratio in the M sites is proportional to and independent of the Fe/Mg ratio of the pyroxene at constant temperature.

The melt-component activities incorporated in calculations of the equilibrium constant (K_{ex}) for the REE exchange reaction:

$$K_{ex} = \left[\frac{X^{cpx}_{REE} X^{cpx}_{Fe} (a^{liquid}_{CaO})(a^{lilquid}_{MgO})(a^{liquid}_{SiO_2})}{X^{cpx}_{Ca} X^{cpx}_{Mg} (a^{liquid}_{AlO_{1.5}})(a^{liquid}_{REEO_{1.5}})(a^{liquid}_{FeO})}\right] \quad (5)$$

were determined assuming the two-lattice melt model. The activity of the mineral components were calculated as the product of the mole fraction of the components in their sites. All REE and Ca were assumed exclusively to occupy the M2 site. The mole fraction of Fe and Mg in the M1 site was assumed to be proportional to the Fe/mg ratio as noted above. Therefore, given these assumptions, the mole fraction of REE, Ca, Fe or Mg in the M1 site is simply four times the mole fraction of the cations in the pyroxene.

To evaluate the effectiveness of K_{ex} at predicting the dependence of REE partitioning on the Ca content of the pyroxene, values for K_{ex} were calculated for the data and plotted versus Ca (Fig. 5). The results show that the dependence is removed for all three data sets, with similar values for orthopyroxene, pigeonite and sub-calcic augite. In addition, the experiments cover a range of temperature from 1050–1400° C. The correlation of the Colson data (1400° C) with data from 1080–1170° C (McKay 1989 and this study) suggests that the temperature dependence is small. A simple measure of K_{ex} may then be calculated as an average of all K_{ex} values in the data sets. These averages (Table 3), calculated from different data sets produce results that are consistent both in continuity between elements and for values calculated from different data sets for the same elements. For example, the averages for K_{ex} for Sm are 0.107 and 0.115 for this study and McKay et al. (1986a) respectively and agree within analytical error. In addition, the value for Yb calculated from McKay et al. (1986a) is 0.276 whereas the value calculated from this study for Ho is 0.325 and for Lu is 0.254. The values for La are 0.033 and 0.012 for this study and McKay et al. (1986a) respectively. The difference in values may be related to the fact that the average crystal sizes in the experiments described here are smaller than those reported by

McKay et al. (1986a), increasing the average amount of glass fluorescence. Alternatively, the difference may simply be related to the larger analytical error at the concentration levels represented in the experiments, or to the effect of temperature.

Table 3. Calculated equilibrium constants for reaction 4. Expressions were calculated based on data reported in this paper, and from data reported by McKay et al. 1986a. Error is expressed in terms of 1σ standard deviations

	This study		McKay et al.	
	Average	Error	Average	Error
La	0.033	0.01	0.012	0.015
Ce			0.022	0.018
Nd			0.077	0.024
Sm	0.107	0.013	0.115	0.011
Gd	0.144	0.017		
Ho	0.325	0.035		
Yb			0.276	0.019
Lu	0.252	0.013		
Y	0.294	0.031		
Sc	3.248	0.406		

Olivine

In a study of Sc partitioning in olivine in a synthetic system, Colson et al. (1989) suggested two possible mechanisms for incorporating Sc into the olivine structure. The first was a paired substitution with Al, replacing a Mg and a Si. The other was a paired substitution of two Sc atoms and a vacancy for three Mg atoms in octahedral sites. To discriminate between these hypotheses, he plotted the Sc and Al mole fractions in the olivine against one another. A correlation with a slope of one would suggest a paired substitution with Al. A slope greater than one would suggest a substitution with a vacancy. We have combined our data set (Table 4) with that of Colson et al. (1988) (Fig. 6) and looked for the same correlation. The results indicate a strong preference in both data sets for a substitution involving two Sc and a vacancy, particularly at high Sc concentrations. This is consistent with the idea that with increasing addition of Sc and vacancies, the lattice becomes increasingly distorted, allowing more Sc and vacancies to be accommodated. Analysis of melt inclusions, or the fluorescence of surrounding glass would have the effect of increasing

Table 4. Experimentally determined olivine and glass compositions. All concentrations are expressed in terms of cation normalized mole percent

systems	Temp		Na	Mg	Al	Si	P	K	Ca	Sc	Ti	Mn	Fe	Y	La
H87-3	1180	olivine	0.0(0)	56.9(4)	0.1(0)	33.4(2)	0.0(0)	0.0(0)	0.4(0)	0.12(2)	0.0(0)	0.16(3)	9.0(2)	0.00(0)	0.00(0)
		glass	4.0(2)	11.1(1)	15.8(2)	46.8(4)	0.5(1)	0.6(1)	12.5(4)	0.54(8)	1.9(2)	0.14(3)	5.9(1)	0.00(0)	0.16(2)
H87-3	1180	olivine	0.0(0)	54.6(5)	0.2(0)	33.4(3)	0.0(0)	0.0(0)	0.4(0)	0.23(3)	0.0(0)	0.15(3)	10.9(2)	0.00(0)	0.00(0)
		glass	3.9(1)	10.5(1)	15.1(3)	45.1(4)	0.2(1)	0.7(1)	12.8(4)	1.08(6)	1.9(2)	0.13(3)	8.2(2)	0.01(0)	0.27(3)
H87-3	1150	olivine	0.0(0)	48.3(4)	0.1(0)	33.3(2)	0.0(0)	0.0(0)	0.3(0)	0.40(6)	0.0(0)	0.17(3)	18.2(4)	0.00(0)	0.00(0)
		glass	4.8(2)	9.9(1)	16.1(4)	45.3(4)	0.3(1)	0.8(1)	11.9(4)	0.60(9)	2.2(3)	0.14(3)	8.4(2)	0.00(0)	0.01(0)
H87-3	1150	olivine	0.0(0)	50.1(3)	0.1(0)	33.1(3)	0.0(0)	0.0(0)	0.4(0)	0.23(3)	0.0(0)	0.18(4)	17.8(4)	0.00(0)	0.00(0)
		glass	4.5(3)	9.2(3)	15.7(3)	45.6(4)	0.3(1)	1.0(1)	11.8(4)	0.61(9)	2.3(3)	0.19(4)	8.8(2)	0.01(0)	0.42(5)
H87-3	1150	olivine	0.0(0)	53.3(6)	0.1(0)	33.5(4)	0.0(0)	0.0(0)	0.3(0)	0.40(6)	0.0(0)	0.17(3)	12.6(3)	0.00(0)	0.00(0)
		glass	4.8(2)	9.9(1)	16.1(2)	45.3(4)	0.3(1)	0.8(1)	12.0(4)	1.51(3)	2.1(2)	0.15(3)	7.4(1)	0.00(0)	0.01(0)
H87-3	1150	olivine	0.0(0)	52.1(3)	0.1(0)	33.1(2)	0.0(0)	0.0(0)	0.4(0)	0.23(3)	0.0(0)	0.18(4)	13.9(3)	0.00(0)	0.00(0)
		glass	4.6(2)	9.1(3)	15.2(4)	45.8(4)	0.3(1)	1.0(1)	11.3(3)	1.23(8)	2.4(3)	0.16(3)	8.9(2)	0.01(0)	0.40(5)
H87-3	1150	olivine	0.0(0)	52.0(2)	0.1(0)	32.9(5)	0.0(0)	0.0(0)	0.4(0)	0.24(4)	0.0(0)	0.17(3)	14.3(3)	0.00(0)	0.00(0)
		glass	4.7(1)	9.1(1)	15.1(3)	45.7(4)	0.3(1)	1.0(1)	11.3(3)	1.34(2)	2.4(3)	0.14(3)	9.1(2)	0.02(0)	0.36(4)
H87-3	1150	olivine	0.0(0)	53.7(4)	0.2(0)	33.6(2)	0.0(0)	0.0(0)	0.4(0)	0.45(7)	0.0(0)	0.17(3)	11.6(2)	0.00(0)	0.00(0)
		glass	4.6(2)	9.8(2)	15.7(2)	44.1(4)	0.3(1)	0.8(1)	11.5(3)	1.89(8)	2.0(2)	0.13(3)	7.6(2)	1.06(17)	0.69(8)
H87-3	1150	olivine	0.0(0)	54.0(5)	0.2(0)	32.9(3)	0.0(0)	0.0(0)	0.4(0)	0.51(8)	0.0(0)	0.14(3)	12.0(2)	0.00(0)	0.00(0)
		glass	4.1(1)	9.8(1)	14.9(2)	44.0(4)	0.2(1)	0.7(1)	12.3(4)	2.28(4)	1.9(2)	0.12(2)	7.9(2)	1.09(17)	0.62(7)
H87-3	1150	olivine	0.0(0)	52.7(3)	0.2(0)	33.4(3)	0.0(0)	0.0(0)	0.3(0)	1.20(8)	0.0(0)	0.16(3)	12.0(3)	0.00(0)	0.00(0)
		glass	4.5(3)	9.5(2)	15.5(4)	43.0(4)	0.3(1)	0.9(1)	9.3(3)	4.12(6)	2.0(2)	0.14(3)	8.5(2)	0.00(0)	2.16(26)
E-1	1100	olivine	0.0(0)	51.8(6)	0.1(0)	33.6(5)	0.0(0)	0.0(0)	0.2(0)	0.48(7)	0.0(0)	0.19(4)	13.6(3)	0.00(0)	0.00(0)
		glass	4.9(5)	7.2(1)	14.0(2)	50.1(5)	0.7(2)	1.9(2)	7.3(2)	1.60(4)	2.4(3)	0.11(2)	6.9(1)	2.21(35)	0.76(9)
E-1	1100	olivine	0.0(0)	50.1(5)	0.3(0)	33.3(3)	0.0(0)	0.0(0)	0.2(0)	0.50(8)	0.0(0)	0.19(4)	15.5(3)	0.00(0)	0.00(0)
		glass	4.7(2)	7.6(2)	13.6(3)	49.6(4)	0.8(2)	1.7(1)	7.6(2)	1.67(5)	2.4(3)	0.13(3)	7.6(2)	2.09(33)	0.73(9)
E-1	1100	olivine	0.0(0)	50.8(4)	0.2(0)	33.2(4)	0.0(0)	0.0(0)	0.2(0)	0.50(8)	0.0(0)	0.21(4)	14.8(3)	0.00(0)	0.00(0)
		glass	5.1(3)	7.5(2)	13.9(2)	49.3(4)	0.6(2)	1.5(1)	7.4(2)	1.75(6)	2.4(3)	0.10(2)	7.7(2)	2.03(32)	0.85(10)
E-1	1100	olivine	0.0(0)	51.3(5)	0.1(0)	33.0(2)	0.0(0)	0.0(0)	0.2(0)	0.71(7)	0.0(0)	0.23(5)	14.4(3)	0.00(0)	0.00(0)
		glass	5.9(4)	7.3(1)	13.9(1)	50.5(5)	0.3(1)	1.0(1)	6.5(2)	2.03(6)	2.3(3)	0.13(3)	7.2(1)	2.06(33)	0.95(11)
E-1	1100	olivine	0.0(0)	50.2(4)	0.2(0)	33.5(3)	0.0(0)	0.0(0)	0.3(0)	0.65(5)	0.0(0)	0.21(4)	15.0(3)	0.00(0)	0.00(0)
		glass	5.1(2)	7.3(3)	13.9(2)	50.0(5)	0.5(1)	1.2(1)	7.1(2)	1.63(4)	2.4(3)	0.16(3)	7.5(1)	2.30(37)	0.90(11)
TLW67	1100	olivine	0.0(0)	44.5(2)	0.1(0)	32.9(3)	0.0(0)	0.0(0)	0.2(0)	0.65(8)	0.0(0)	0.22(4)	21.4(4)	0.00(0)	0.00(0)
		glass	4.3(3)	7.1(1)	12.9(3)	47.5(2)	0.3(1)	1.1(1)	8.1(2)	2.22(9)	3.2(4)	0.18(4)	11.0(2)	1.24(20)	0.68(8)
2MH005	1120	olivine	0.0(0)	49.2(5)	0.2(0)	32.9(5)	0.0(0)	0.0(0)	0.3(0)	0.84(13)	0.0(0)	0.25(5)	16.2(3)	0.00(0)	0.00(0)
		glass	5.3(2)	7.7(3)	15.8(2)	45.8(2)	0.6(2)	1.9(1)	8.0(2)	2.61(9)	1.6(2)	0.16(3)	8.5(2)	1.24(20)	0.96(12)
2MH005	1090	olivine	0.0(0)	45.4(2)	0.1(0)	32.9(3)	0.0(0)	0.0(0)	0.3(0)	0.69(8)	0.0(0)	0.33(7)	20.3(4)	0.00(0)	0.00(0)
		glass	5.3(1)	6.0(2)	15.3(1)	46.5(5)	0.8(2)	2.3(2)	7.4(2)	2.05(3)	1.9(2)	0.22(4)	9.6(2)	1.52(24)	1.28(15)
2MH005	1090	olivine	0.0(0)	45.4(3)	0.2(0)	32.8(5)	0.0(0)	0.0(0)	0.3(0)	0.80(6)	0.0(0)	0.33(7)	20.2(4)	0.00(0)	0.00(0)
		glass	5.4(2)	6.0(1)	15.3(3)	46.3(3)	0.8(2)	2.1(2)	7.5(2)	2.07(3)	2.0(2)	0.19(4)	9.3(2)	1.55(25)	1.42(17)

the Al content at any fixed Sc content, and thereby making the correlation appear to be closer to 1:1.

Utilizing this information, we can calculate an approximate equilibrium constant (K′) based on the reaction:

$$2Sc_2O_3(\text{liquid}) + 3SiO_2(\text{liquid}) = Sc_4 \quad {}_2Si_3O_{12}. \quad (6)$$

Determining the activity of the Sc olivine component is complicated by the effect of the vacancy on the olivine-component activity. For the purpose of these calculations, the activity of the Sc olivine component is assumed equal to the mole fraction of Sc in the olivine. The activity of melt components was calculated assuming the two-lattice melt model. The results of the calculations (Fig. 7) indicate both that there is a significant temperature effect and that the trends represented in the Colson et al. (1988) data are consistent with our new data on terrestrial compositions.

The results of our analyses of REE partitioning between olivine and melt produced values for D_{REE} (Table 5) that were similar to, but slightly higher than those determined by McKay (1986). This may be due to the effect of melt composition, or because of increased fluorescence of the surrounding glass related to a smaller mean crystal size in our experiments. The characteristic low D_{La} and D_{Sm} are still evident. Therefore the models based upon the partitioning data of McKay (1986) are still valid (e.g. Keleman et al. 1990). By inference from the Sc partitioning data, we can expect that there is a significant effect of temperature and melt composition on REE partitioning. However, because of the extremely low concentrations of REE in these charges, analytical error is larger, and would mask any such dependence.

Given that the elements of interest have a valence of +3, and the generally presumed reluctance of olivine to accommodate them in its structure, we paid particular attention to any observable dependence of partitioning on concentration (possible Henry's law violation). An ankaramite starting composition was doped with 5 different levels of Sc. All were run for the same time period and temperature 1150° C, at the QFM buffer and quenched in water (Fig. 8). There is a significant increase in both D and K′ at concentrations above 2 cation normalized mol% Sc in the melt. We interpret this as a significant positive departure from Henry's Law behavior. This suggests that as more Sc is taken into the structure of the olivine, the capability of the crystal structure to accommodate the element is enhanced.

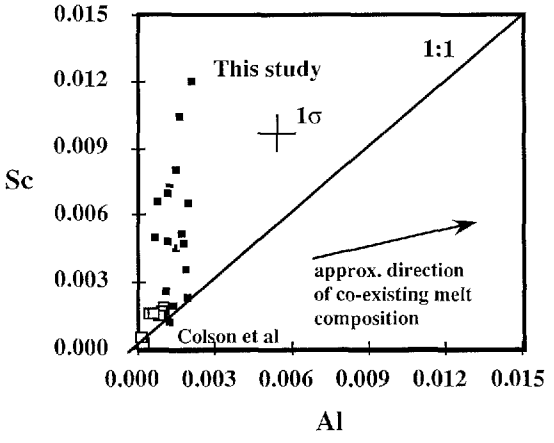

Fig. 6. Correlation of Sc and Al mole fractions in olivine. *Line* represents a 1:1 relationship

Table 5. Partition coefficients determined for olivine, magnetite and ilmenite by long-count-time analysis. Values represent averages of multiple analyses on several different samples. The number of samples in the average is given in parentheses. 1σ precisions are given in parentheses (0.0072(19) is 0.0072 ± 0.0019). These are calculated on the basis of multiple determinations

	Olivine (6)	Magnetite (5)	Ilmenite (4)
La	<0.0001	0.0029(15)	0.0072(19)
Sm	0.0011(5)	0.0072(15)	0.0091(11)
Gd	0.0029(12)	0.0055(12)	0.0077(13)
Ho	0.013(5)	0.0079(17)	0.012(4)
Lu	0.051(5)	0.023(4)	0.029(3)
Y	0.0036(12)	0.0039(17)	0.0045(9)

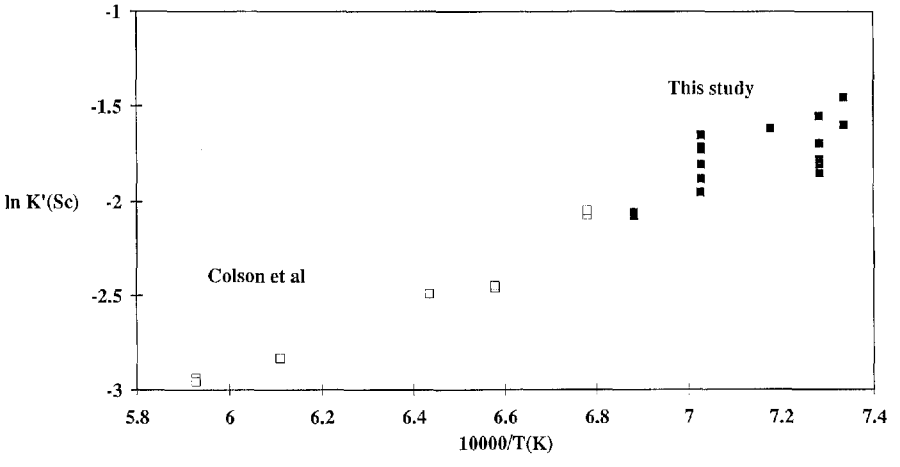

Fig. 7. Correlation of the equilibrium constant for a Sc olivine crystallization reaction with reciprocal temperature

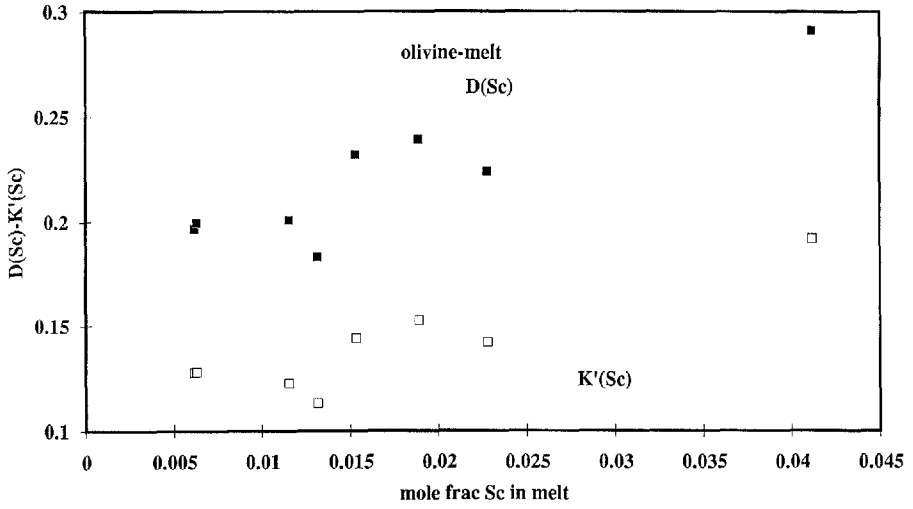

Fig. 8. Olivine-melt partition coefficient and K′ (equilibrium constant) for Sc as a function of Sc concentration in the melt

Magnetite and ilmenite

Of the mineral phases considered in this study, the oxides have by far the least amount of published experimental partitioning information available. In the case of magnetite we could find no experimentally determined values in the literature. For ilmenite, there is only one determination, that by McKay et al. (1986b). The available oxide/matrix values for D_{REE} have a range of 2–3 orders of magnitude (Fig. 9). Such a range of equilibrium values is not impossible, particularly given the range of experimental values for high-field-strength elements (Zr, Hf, Ta, Nb, V) magnetite-melt partition coefficients (Nielsen et al. 1990). Using a modified version of the technique of McKay (1986), five charges were analyzed for magnetite and four for ilmenite. The magnetites ranged in composition from high-Al (~8 wt% Al_2O_3) magnetite, to titanomagnetite to almost pure (Fe, Mg) magnetite. The relatively narrow range of partition coefficients (Table 5) show that there is relatively little effect of mineral composition on the partitioning behavior of REE for either magnetite or ilmenite. Again, because of the low concentration of REE in the mineral phases (50–300 ppm), analytical error is almost certainly larger than any compositional or temperature dependence. The ilmenite-melt value of McKay et al. (1986b) is within the range of values determined from the charges produced for this study. The observed differences between the experimentally determined values of partition coefficients and most phenocryst-matrix partition coefficients suggest that the phenocryst/matrix values are unreliable, probably because of inclusions in the separated minerals.

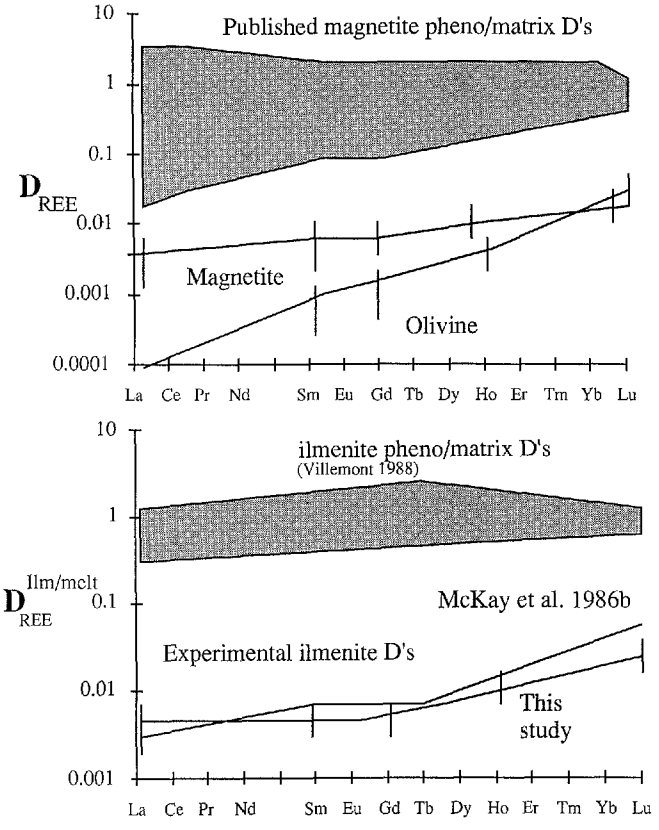

Fig. 9. Comparison of published phenocryst/matrix partition coefficients with experimental determinations from McKay et al. (1986b) and this study. Olivine-melt D_{REE} is an average of 4 determinations made in this study on results from H-87-3 at 1150° C, E-1 at 1100° C, GC-68 at 1100° C and 45321 at 1080° C. *Vertical bars* represent the 1σ standard deviation on these multiple determinations. Magnetic phenocryst/matrix values are from Lemarchande et al. (1987), Villemant (1988), Worner et al. (1983) and Schock (1979)

Conclusions

To describe better the partitioning behavior of the trivalent cations Sc, Y and the REE we conducted a series of experiments on natural composition lavas. As reported by McKay et al. (1986a), there is a strong correlation between Y, Sc and REE partitioning and the Ca content in pyroxene. By defining a mineral-melt expression based on an exchange reaction, it is possible to calculate a compositionally independent term (K_{ex}) that can be used to describe pyroxene-melt partitioning behavior for a wide range of mineral and melt composition.

In general, Sc substitutes into olivine in a paired substitution of two Sc atoms and a vacancy for three Mg or Fe atoms. There may be an additional effect of minor Sc–Al paired substitution. The partitioning of Sc is dependent both on melt composition and temperature. Olivine-melt REE Ds are similar to, but slightly higher than the results reported by McKay (1986). Our results support the conclusions of McKay (1986) that olivines are strongly LREE depleted.

Y and REE mineral/melt partition coefficients for magnetite range from 0.003 for La to 0.02 for Lu. Ilmenite partition coefficients range from 0.007 for La to 0.029 for Lu. These experimental values are two orders of magnitude lower than many of the published values determined by phenocryst/matrix separation techniques.

Acknowledgements. We wish to thank T. Wright, W. Leeman, M. Rhodes, W. Melson, R. Tilling, and D. Baker for graciously providing samples used as our experimental systems. Discussions and reviews by Gordon McKay, Russ Colson and the basalt bunch at OSU provided valuable insight which improved this work considerably. This project was made possible by funding through NSF grants EAR 87-20683 and EAR 90-03930 to R.L. Nielsen.

References

Beattie PD (1991) Incompatible element partition coefficients for olivine-melt and orthopyroxene-melt systems. EOS 72:318

Bottinga Y, Weill DF (1972) The viscosity of magmatic silicate liquids: a model for calculation. Am J Sci 272:438–475

Casadevall TJ, Dzurisin D (1987) Stratigraphy and petrology of the Uwekahuna Bluff section, Kilauea caldera. In: Decker RW, Wright TL, Stauiffer PH (eds) Volcanism in Hawaii. US Geol Surv Prof Pap 1350, pp 351–376

Colson RO, McKay GA, Taylor LA (1988) Temperature and composition dependencies of trace element partitioning: olivine/melt and low-Ca pyroxene/melt. Geochim Cosmochim Acta 52:539–553

Colson RO, McKay GA, Taylor LA (1989) Charge balancing of trivalent trace elements in olivine and low-Ca pyroxene: a test using experimental partitioning data. Geochim Cosmochim Acta 53:643–648

Dunn T (1987) Partitioning of Hf, Lu, Ti, and Mn between olivine, clinopyroxene and basaltic liquid. Contrib Mineral Petrol 96:476–484

Gallahan WE, Nielsen RL (in press) Experimental determination of the partitioning of Sc, Y and REE between high-Ca clinopyroxene and natural mafic liquids. Geochim Cosmochim Acta

Keleman PB, Johnson KTM, Kinzler RJ, Irving AJ (1990) High field strength element depletions in arc basalts die to mantle-magma interaction. Nature 345:521–524

Johnson KTM (1989) Partitioning of REE, Ti, Zr, Hf, and Nb between clinopyroxene and basaltic liquid: an ion microprobe study. EOS Trans Am Geophys Union 70:1388

Kring DA, McKay GA (1984) Chemical gradients in glass adjacent to olivine in experimental charges and Apollo 15 green glass vitrophyres. Lunar Planet Sci XV:461–462

Kuno H (1950) Petrology of Hakone Volcano and the adjacent areas, Japan. Geol Soc Am Bull 61:957–1020

Leeman WP (1974) Experimental determination of partitioning of divalent cations between olivine and basaltic liquid. PhD Thesis, Univ Oregon, Eugene

Lemarchande F, Benoit V, Calais G (1987) Trace element distribution coefficients in alkaline series. Geochim Cosmochim Acta 51:1071–1081

Lindstrom DJ (1976) Experimental study of the partitioning of the transition metals between clinopyroxene and coexisting silicate liquids. PhD Thesis, Univ Oregon, Eugene

McKay GA (1986) Crystal/liquid partitioning of REE in basaltic systems: extreme fractionation of REE in olivine. Geochim Cosmochim Acta 50:69–79

McKay GA (1989) Partitioning of rare earth elements between major silicate minerals and basaltic melts. In: Lipin BR, McKay GA (eds) Geochemistry and mineralogy of rare earth elements (Reviews in Mineralogy 21). Mineral Soc Am, Washington, D.C., pp 45–78

McKay GA, Wagstaff J, Yang S-R (1986a) Clinopyroxene REE distribution coefficients for shergottites: the REE content of the Shergotty melt. Geochim Cosmochim Acta 50:927–937

McKay GA, Wagstaff J, Yang S-R (1986b) Zirconium, halfnium and rare earth element partition coefficients for ilmenite and other minerals in high-Ti lunar mare basalts: an experimental study. Proc 16th, Lunar Planet Sci Conf Geophys Res 91:D229–D237

Moore RB, Helz RT, Dzurisin D, Eaton GP, Koyanagi RY, Lipman PW, Lockwood JP, Puniwai GS (1980) The 1977 eruption of Kilauea volcano, Hawaii. J Volcanol Geothermal Res 7:189–210

Neal CA, Duggan TJ, Wolfe EW, Brandt EL (1988) Lava samples, temperatures, and compositions. In: Wolfe EW (ed) The Puu Oo eruption of Kilauea volcano, Hawaii: episodes 1 through 20, January 3, 1983, through June 8, 1984. US Geol Surv Prof Pap 1463, pp 99–126

Nielsen RL (1985) A method for the elimination of the compositional dependence of trace element distribution coefficients. Geochim Cosmochim Acta 49:1775–1779

Nielsen RL (1988) A model for the simulation of combined major and trace element liquid lines of descent. Geochim Cosmochim Acta 52:27–38

Nielsen RL, Fisk MR, Gallahan WR (1990) Partitioning behavior of Zr, Nb, Hf, Ta, Th, and U between magnetite and natural mafic silicate magma (abstract). Geol Soc Am Abstr Program 22:A255

Porter SC, Garcia MO, Lockwood JP, Wise WS (1987) Guidebook for Mauna Loa-Mauna Kea-Kohala field trip. Hawaii symposium on how volcanoes work

Ray GL, Shimizu N, Hart SR (1983) An ion microprobe study of the partitioning of trace elements between clinopyroxene and liquid in the system diopside-albite-anorthite. Geochim Cosmochim Acta 47:2131–2140

Rhodes JM (1988) Geochemistry of the 1984 Mauna Loa eruption: implications for magma storage and supply. J Geophys Res 93:4453–4466

Roeder PL, Emslie RF (1970) Olivine-liquid equilibrium. Contrib Mineral Petrol 29:275–289

Schock HH (1979) Distribution of rare earth and other trace elements in magnetites. Chem Geol 26:119–133

Villemant B (1988) Trace element evolution in the Plegrean Fields (Central Italy): fractional crystallization and selective enrichment. Contrib Mineral Petrol 98:169–183

Watson EB (1985) Henry's law behavior in simple systems and in magmas: criteria for discerning concentration-dependent partition coefficients in nature. Geochim Cosmochim Acta 49:917–923

Williams RJ, Mullins O (1981) JSC systems using solid ceramic oxygen electrolyte cells to measure oxygen fugacities in gas mixing systems. NASA TMX-58234

Wright TL, Fiske RS (1971) Origin of the differentiated and hybrid lavas of Kilauea volcano, Hawaii. J Petrol 12:1–65

Worner G, Beusen JM, Duchateau N, Gijbels R, Schmincke HU (1983) Trace element abundances and mineral/melt distribution coefficients in phonolites from the Laacher See Volcano (Germany). Contrib Mineral Petrol 84:152–173

Editorial responsibility: T.L. Grove